Development of a Composite I.P.R. Model for Multi-Layered Reservoirs

Pepple, Cyril Christopher¹, Ezenworo, Ebuka Johnmary²
¹(Petroleum & Gas Engineering, University of Port Harcourt, Nigeria)
²(Petroleum & Gas Engineering, University of Port Harcourt, Nigeria)

ABSTRACT: Inflow performance relationship (IPR) is one of the most important tools used to predict performance of oil wells. Most of the present methods used for predicting IPR's are idealistic as they do not take into account the varying permeability that exist in real reservoir systems. As a result of the foregoing, there is a need for IPR models that are representative of real reservoir systems instead of idealized reservoir systems. This study takes into account the effects permeability variation in reservoir layers can have on IPR curves. Multiphase flow in multilayer reservoirs was analyzed and the fluid flow equation for a solution gas drive system presented. Data were then simulated using a computer model (computer program) that was developed on C# interface based on the derived equations. The simulated data were then used to obtain IPR plots. The coefficients obtained from the IPR plots formed the basis of the new correlation development. The two-phase correlation generated from the IPR plots can be applied to optimally improve field development strategy. This, however is because it was tested against other already-established correlations using a field case.

KEYWORDS -Composite, I.P.R., model, mathematics, reservoir

I. INTRODUCTION

Inflow Performance Relationship (IPR), one of the important tools used by the Production Engineer, is an analytical relationship between bottom-hole pressure and production rate formulated for a given flow regime. These flow regimes on which reservoir deliverability can be mathematically modelled can be either transient state flow, steady-state flow, or pseudo-steady state flow regimes.

In the transient state flow regime, the radius of pressure wave propagation from the wellbore has not reached the boundaries of the reservoir, making the reservoir to act like an infinitively large reservoir. In the steady-state flow regime, the pressure at any point in the reservoir remains constant over time since the pressure funnel has propagated to a constant pressure boundary. However, in the pseudo-steady state flow regime, the pressure at any point in the reservoir declines at the same rate over time since the pressure funnel has now propagated to no-flow boundaries.

To better understand IPR, the IPR curve, which is a graphical relationship between the bottom-hole flowing pressure and the liquid production rate, is frequently utilized. The IPR curve is constructed using either inflow models which can be empirically or theoretically based or using test points.IPR modelling can also be extended to situations in which the vertical wellbore in the production zone has different layers having different reservoir pressures, permeability, and producing fluids. This situation is known as a multi-layered or stratified reservoir system.

A multi-layer system is usually described for situations in which there is flow of fluids from one reservoir layer to the other. This phenomenon in which there is flow between the layers is known as inter-layer cross-flow. There are also situations in which there is no cross-flow between layers, the only interaction among layers being via the vertical wellbore drilled across the stratified reservoir. In this case, there exists a barrier between each of the

layers, preventing inter-layer cross-flow from occurring. In no cross-flow situations, most of the production will come from the most permeable layers. IPR of multi-layered reservoirs can be modelled compositely for both cross-flow and no cross-flow situations.

Many research works have been presented to understand the IPR of several reservoir conditions.

A study of the rate-time and pressurecumulative production depletion performance of a two-layered gas reservoir producing without formation cross-flow was carried out by Fetkovich et al., (1990). The gas reservoir they studied had produced for about 20 years at an effectively constant wellbore pressure and had thus given continuously declining rate-time and pressurecumulative production data that were used for analysis. The field data they studied demonstrated that Arps depletion-decline exponents between 0.5 and 1 could be obtained with a no cross-flow, layered reservoir description. Also, rate-time and pressure-cumulative productions predictions were developed in their research work from both 2D numerical simulation and simplified tank models of a two-layered, no cross-flow system. The results they obtained showed the effects of changes in layered volumes of the reservoir, permeability and skin on the depletion performance.

In the research work presented by Daoud et al. (2017), correlations used in modelling IPR were classified into empirically-derived and analytically derived. The empirically-derived were seen to be those derived from data from simulation operations or field operations. However, basic principle of mass balance that describe multiphase flow within the reservoir were seen to be the source of the analytically-derived correlations. The limited ranges of data used in the generation of the empirical correlations was seen as one of the cons of the empirical correlations and also, they do not depend on the petro-physical data that vary for each reservoir. One of the cons of the analytically-derived correlations is the difficulty in obtaining the input data required for them to be applied. Daoud et al. (2017) used a 3D radial single well simulation model to study the effects of a wide range of rock and fluid properties on the IPR for solution gas-drive reservoirs. They then generated a general IPR correlation that functions for highly sensitive rock and fluid data. They used more than 500 combinations of rock and fluid properties to generate different IPRs. A distinct parameter representing each IPR was then gotten using non-linear regression. A non-parametric regression was then utilized to obtain the general IPR correlation. For validation of this general IPR correlation, it was tested on synthetic and field cases. The results of their research showed the extent to which their correlation could be applied compared to previous incompetent correlations.

Milad et al. (2013) modelled and simulated commingled production from multilayered reservoirs containing shale-gas. They were also able to obtain a picture of the pressure and flowrate of the reservoir by simulation. In their work, an iterative numerical simulation scheme was developed for calculations of reservoir hydraulics and coupled wellbore for multilayered shale-gas bearing reservoirs. Case studies were used to evaluate the performance of each layer of the reservoir communicating with the wellbore, both in scenarios of formation cross-flow and no formation cross-flow. In their work, apparent gas permeability in shale, based on pore proximity effects, was considered in other to account for changes in the shale permeability with the prevailing conditions in the formation. The simulation method presented by Milad et al. (2013) enabled an accurate pressure and production evaluation at each layer including formation cross-flow effects.

Guo et al. (2006) derived a composite IPR model for multi-lateral wells. Their paper presented a more accurate method for predicting composite IPR of multi-lateral wells since well planners had, over the years, estimated wrongly the productivity of wells using inaccurate methods.

Elias et al. (2009) developed a new model to predict IPR curve, using a new correlation that accurately describes the behaviour of the oil mobility as a function of the average reservoir pressure.

Qasem et al. (2012a) published a thorough investigation on IPR curves for solution gas-drive reservoirs. They presented an IPR equation that predicts accurately well performance under different depletion scenarios. They also presented an equation that forecasts future IPR behaviour. The IPR equations presented by Qasem et al. (2012a) are applicable for wells producing from two-layer systems without fluid cross flow.

Afterward, Qasem et al. (2012b) presented a preliminary study for two and multi-layer solution

gas-drives with fluid cross flow. The latter study showed that the IPR curves for these types of reservoirs have peculiar shapes and needed to be investigated further.

There is an urgent need to model the IPR of wells producing from multi-layered reservoirs for fluid cross-flow situations. This research work provides comprehensive coverage of the above scenario.

The body of this papercomprises of three (2) main sections as follows;

Methodology: Gives a detailed description of the model and simulation done with respect to the inflow performance relationship of multi-layered reservoirs.

Results and Discussions: Shows the details of the result obtained on completion of the modelling.

Conclusion: Summarizes the research work and includes contributions to knowledge.

II. METHODOLOGY

2.1. Development of Multi-Layered Reservoir Model Considering Multiphase Fluid Flow

Modelling multi-layered reservoirs are pertinent in minimizing the uncertainty of production from each layer. Here, differences in rock and fluid properties in the layers are put into account just like in field cases, instead of the usual averaging of the parameters for all reservoir layers (Milad et al., 2013). Understanding the concepts behind any computer model that would be used in simulating the reservoir properties for a multi-layered system would be helpful in obtaining proper insight into the reservoir behavior and in IPR data acquisition.

2.2. Assumptions Considered

For the analytic consideration of the above, certain general assumptions were made. Such as:

- The reservoir pressure is at the bubble-point pressure and there is an existence of a gas coming out of the liquid phase, instigating twophase flow - the gas is dissolved in the oil;
- A small element, a control volume in the multilayer system is taken out for detailed study;
- A cylindrical coordinate system is assumed since the main intent of this research work is to model inflow performance into the wellbore.
- Flow in the vertical permeability section of the

- control volume amongst the layers of the reservoir is taken as the z-direction of the coordinate system;
- Flow into and out of the control volume is seen as flow in the radial direction with the tangential flow effects being neglected since they do not contribute to the conservation of mass relationship.
- No fluid flow occurs at the outer reservoir boundary;
- The reservoir is at isothermal conditions with thermodynamic equilibrium attained all through the reservoir;
- 2.3. Multiphase Flow Equations in a Black Oil Reservoir Using the Law of Conservation of Mass

Considering a Control Volume (CV). There is no injection nor production from the control volume, just mass transferred in and mass transferred out.

The concept of material balance can be written as:

(Rate of Mass entering CV)(Rate of Mass leaving CV)
= (Rate of Mass stored in CV)(2.1)

Where:

Rate of Mass entering
$$CV = \rho q|_r(2.2)$$

Rate of Mass leaving $CV = \rho q|_{r+\Delta r}(2.3)$
Rate of Mass stored in CV , $\dot{m} = \frac{\partial}{\partial t}(2\rho\phi\pi rh\Delta r)(2.4)$

Substituting (2.2), (2.3) and (2.4) into (2.1):

$$\rho q|_{r} - \rho q|_{r+\Delta r} = \frac{\partial}{\partial t} (2\rho \phi \pi r h \Delta r)(2.5)$$

From Taylor's series expansion when higher derivatives are neglected,

$$\rho q|_{r+\Delta r} = \rho q|_r + \Delta r \frac{\partial(\rho q)}{\partial r}|_r (2.6)$$

Substituting (2.6) into(2.5):

$$\rho q|_{r} - \left(\rho q|_{r} + \Delta r \frac{\partial(\rho q)}{\partial r}|_{r}\right) = \frac{\partial}{\partial t} (2\rho \phi \pi r h \Delta r)(2.7)$$

By opening the brackets on the left hand-side and simplifying, eqn. (2.7) becomes:

$$-\left(\Delta r \frac{\partial(\rho q)}{\partial r}|_{r}\right) = \frac{\partial}{\partial t} (2\rho \phi \pi r h \Delta r)(2.8)$$

(2.8) is the general continuity equation in cylindrical coordinates.

Accounting for flow in the vertical direction, (2.8) becomes:

$$-\Delta r \frac{\partial (\rho q_r)}{\partial r}|_r - \Delta z \frac{\partial (\rho q_z)}{\partial r}|_z = \frac{\partial}{\partial t} (2\rho \phi \pi r h \Delta r) (2.9)$$

But,

$$q_r = \frac{-2\pi \mathrm{rh}k}{\mu} \frac{\partial P}{\partial r} (2.10)$$

And

$$q_z = \frac{-2\pi r \Delta r k}{\mu} \frac{\partial P}{\partial r} (2.11)$$

Substituting (2.10) and (2.11) into(2.9) and eliminating like terms:

$$\frac{2\pi kh}{\mu}\frac{\partial}{\partial r}\left(r\frac{\partial P}{\partial r}\right) + \frac{2\pi rk\Delta z}{\mu}\frac{\partial}{\partial z}\left(\frac{\partial P}{\partial z}\right) = 2\pi rh\frac{\partial\phi}{\partial r}(2.12)$$

Porosity as a function of pressure is given as:

$$\phi = \phi^o [1 + C_f (P - P^o)] (2.13)$$

Differentiating eqn. (2.13) w.r.t time, it will result to

$$\frac{\partial \phi}{\partial t} = \frac{\partial}{\partial t} \left[\phi^o + C_f \phi^o (P - P^o) \right] (2.14)$$

The above eqn. then results to:

$$\frac{\partial \phi}{\partial t} = C_f \phi \frac{\partial P}{\partial t} (2.15)$$

Substituting (2.15) into (2.12):

$$\begin{split} \frac{2\pi kh}{\mu} \frac{\partial}{\partial r} \left(r \frac{\partial P}{\partial r} \right) + \frac{2\pi rk\Delta z}{\mu} \frac{\partial}{\partial z} \left(\frac{\partial P}{\partial z} \right) \\ &= 2\pi rh C_f \phi \frac{\partial P}{\partial t} (2.16) \end{split}$$

$$F_r = \frac{2\pi kh}{\mu} (2.17)$$

$$F_z = \frac{2\pi r k \Delta z}{\mu} (2.18)$$

$$V = 2\pi r h C_f \phi(2.19)$$

Substituting (2.17), (2.18) and (2.19) into (2.16):
$$F_r \frac{\partial}{\partial r} \left(r \frac{\partial P}{\partial r} \right) + F_z \frac{\partial}{\partial z} \left(\frac{\partial P}{\partial z} \right) = V \frac{\partial P}{\partial t} (2.20)$$

2.4. Finite Difference Approximations

Discretization of the continuity equation obtained in section (2.3) above utilizes the finite difference approach.

The grid points used are shown in Fig 2.1. (2.20) can be re-written in time and space coordinates using implicit formulation as:

$$\begin{split} F_r \left(r \frac{\partial P^{n+1}}{\partial r} |_{i+1,j} - r \frac{\partial P^{n+1}}{\partial r} |_{i,j} \right) \\ + F_z \left(\frac{\partial P^{n+1}}{\partial z} |_{i,j+1} - \frac{\partial P^{n+1}}{\partial z} |_{i,j} \right) \\ = V \frac{\partial P^{n+1}}{\partial t} |_{i,j} (2.21) \end{split}$$

(2.21) can be discretized in time and space using the Central Difference approach. Applying the Central difference approach to discretize (2.20) results in:

$$\begin{split} F_{r}r\left(\frac{P_{i+1,j}^{n+1}-P_{i,j}^{n+1}}{\Delta r}\right) - & F_{r}r\left(\frac{P_{i,j}^{n+1}-P_{i-1,j}^{n+1}}{\Delta r}\right) + \\ F_{z}\left(\frac{P_{i,j+1}^{n+1}-P_{i,j}^{n+1}}{\Delta z}\right) - & F_{z}\left(\frac{P_{i,j}^{n+1}-P_{i,j-1}^{n+1}}{\Delta z}\right) = \\ V\left(\frac{P_{i,j}^{n+1}-P_{i,j}^{n}}{\Delta t}\right)(2.22) \end{split}$$

(2.22) can be re-arranged as:

$$\begin{split} F_{rE} r_E \left(\frac{p_{i+1,j}^{n+1} - p_{i,j}^{n+1}}{\Delta r} \right) + F_{rW} r_W \left(\frac{p_{i-1,j}^{n+1} - p_{i,j}^{n+1}}{\Delta r} \right) + \\ F_{zN} \left(\frac{p_{i,j+1}^{n+1} - p_{i,j}^{n+1}}{\Delta z} \right) + F_{zS} \left(\frac{p_{i,j-1}^{n+1} - p_{i,j}^{n+1}}{\Delta z} \right) = \\ V \left(\frac{p_{i,j}^{n+1} - p_{i,j}^{n}}{\Delta t} \right) (2.23) \end{split}$$

Where the subscripts 'E', 'W', 'N' and 'S' represent the East, West, North and South directions corresponding to the ' $i^{th}+1$ ', ' $i^{th}-1$ ', ' $j^{th}+1$ ' and 'jth-1' grid points in space respectively. Let:

$$T_W = \frac{F_W r_W \Delta t}{\Delta r} (2.24)$$

$$T_E = \frac{F_{rE} r_E \Delta t}{\Delta r} (2.25)$$

$$T_N = \frac{F_{ZN} \Delta t}{\Delta r} (2.26)$$

$$T_S = \frac{F_{ZS} \Delta t}{\Delta r} (2.27)$$

Substituting (2.24), (2.25), (2.26) and (2.27) into (2.23):

$$T_{E}(P_{i+1,j}^{n+1} - P_{i,j}^{n+1}) + T_{W}(P_{i-1,j}^{n+1} - P_{i,j}^{n+1}) + T_{N}(P_{i,j+1}^{n+1} - P_{i,j}^{n+1}) + T_{S}(P_{i,j-1}^{n+1} - P_{i,j}^{n+1}) = V(P_{i,i}^{n+1} - P_{i,i}^{n})(2.28)$$

For Gas flow, eqn. (2.28) is modified to:

$$T_{Eg}(P_{i+1,j}^{n+1} - P_{i,j}^{n+1}) + R_s T_{Eo}(P_{i+1,j}^{n+1} - P_{i,j}^{n+1}) + T_{Wg}(P_{i-1,j}^{n+1} - P_{i,j}^{n+1}) + R_s T_{Wo}(P_{i-1,j}^{n+1} - P_{i,j}^{n+1}) + T_{Ng}(P_{i,j+1}^{n+1} - P_{i,j}^{n+1}) + R_s T_{No}(P_{i,j+1}^{n+1} - P_{i,j}^{n+1}) + T_{Sg}(P_{i,j-1}^{n+1} - P_{i,j}^{n+1}) + R_s T_{So}(P_{i,j-1}^{n+1} - P_{i,j}^{n+1}) = V(P_{i,j}^{n+1} - P_{i,j}^{n})(2.29)$$

Where:

Rs is the solution GOR, and subscripts 'g' and 'o' stand for gas and oil respectively.

j - Direction	0 i - 1, j+1	0 i -1, j+1	0 i -1, j+1
	0 i -1, j+1	0 i -1, j+1	0 i -1, j+1
	0 i -1, j+1	0 i -1, j+1	0 i -1, j+1

i - Direction

Figure 2.1: Two Dimensional Grid

2.5. Method of Obtaining Solution

There are several methods that could be applied in obtaining the solution to the fluid flow equation for a solution gas-drive reservoir as represented by (2.29), but the method applied for this research work is the Newton-Raphson's scheme for obtaining solutions to non-linear equations.

2.5.1. Newton-Raphson's Method of Solving Non-Linear Equations

The Newton-Raphson's method is one of the well-known approximation methods used in numerical analysis to solve non-linear equations. Newton-Raphson's method is prominent for its fast speed of converging at the best solution; especially when the initial guess is close to the root of the equation sufficiently.

The general form of Newton-Raphson's method is

given as:

$$x_{n+1} = x_n - \frac{f(x_n)}{f'(x_n)}$$
 (2.30)

For a system of non-linear equations, we have:

$$f(x) = 0(2.31)$$

Where x and f are n-vectors

$$x = \begin{pmatrix} x_1 \\ x_2 \\ \vdots \\ x_n \end{pmatrix}; f(x) = \begin{pmatrix} f_1(x_1, x_2, \dots, x_n) \\ f_2(x_1, x_2, \dots, x_n) \\ \vdots \\ f_n(x_1, x_2, \dots, x_n) \end{pmatrix} (2.32)$$

Based on (2.32), (2.30) can be re-written to include the Jacobian Matrix since $f'(x_n)$ in (2.30) takes the form of the Jacobian Matrix.

Re-writing eqn. (2.30) in terms of the Jacobian:

$$x_{n+1} = x_n - \frac{f(x_n)}{J}(2.33)$$

Eqn. (2.33) then becomes:

$$J\Delta x = -f(x_n)(2.34)$$

Where:

$$\Delta x = x_{n+1} - x_n(2.35)$$

$$J = \begin{pmatrix} \frac{df_{1}}{dx_{1}}, & \frac{df_{1}}{dx_{2}}, & \dots & \frac{df_{1}}{dx_{n}} \\ \frac{df_{2}}{dx_{1}} & \frac{df_{2}}{dx_{2}} & \dots & \frac{df_{2}}{dx_{n}} \\ \vdots & \vdots & \ddots & \vdots \\ \frac{df_{n}}{dx_{1}} & \frac{df_{n}}{dx_{2}} & \dots & \frac{df_{n}}{dx_{n}} \end{pmatrix} (2.36)$$

Number of columns in *I*

= Number of unknowns in equation
$$(2.37)$$

Number of rows in *J*

$$=$$
 Number of equations (2.38)

Newton-Raphson's formula is written in terms of Pressure as:

$$J\Delta P_n = -f(P_n)(2.39)$$

$$P_{n} = \begin{pmatrix} P_{1} \\ P_{2} \\ \vdots \\ P_{n} \end{pmatrix}; f(P_{n}) = \begin{pmatrix} f_{1}(P_{1}, P_{2}, \dots, P_{n}) \\ f_{2}(P_{1}, P_{2}, \dots, P_{n}) \\ \vdots \\ f_{n}(P_{1}, P_{2}, \dots, P_{n}) \end{pmatrix} (2.40)$$

Changing notations to represent pressure in the Jacobian matrix:

$$J = \begin{pmatrix} \frac{df(P_1)}{dx_1}, & \frac{df(P_1)}{dx_2}, & \dots & \frac{df(P_1)}{dx_n} \\ \frac{df(P_2)}{dx_1} & \frac{df(P_2)}{dx_2} & \dots & \frac{df(P_2)}{dx_n} \\ \vdots & \vdots & & \vdots \\ \frac{df(P_n)}{dx_1} & \frac{df(P_n)}{dx_2} & \dots & \frac{df(P_n)}{dx_n} \end{pmatrix} (2.41)$$

2.5.2. Model Inputs

The computer model (simulator) would require some inputs in order to obtain the coefficients needed for the IPR modelling and permeability effects on production. Some of these inputs include:

- Bubble-point pressure
- Initial reservoir pressure
- Reference pressure
- Gas gravity, g (dimensionless)
- Initial oil saturation
- Residual oil saturation
- Critical gas saturation
- Connate water saturation
- Oil compressibility
- Rock compressibility
- Formation porosity
- Wellbore radius
- Reservoir drainage radius
- Pay zone thickness
- Reservoir temperature

2.6. Computer Model

The computer model for simulating the reservoir properties was developed using a Windows Presentation Foundation (WPF) application on Microsoft Visual Studio. The coding was done using C# computer programming language. The coding was based on the multiphase fluid flow equation that was derived in sections 2.1 to 2.5 of this research work. Details of coding done on the C# interface are in the Appendix section of this work. However, the output user interface is shown in Figures 2.2, 2.3,

2.4, and 2.5.

Pressure (Psia)	Solution GOR (Scf/Stb)	Oil FVF (Rb/Stb)	Gas FVF (Rb/Scf)	
14.7	103.176	1.13912	0.201988	İ
150.965	132.278	1.15112	0.0193907	1
287.23	156.549	1.16143	0.0100493	1
423.495	180.071	1.17165	0.00672216	T
559.76	203.539	1.18205	0.00501741	t
696.025	227.229	1.19275	0.00398247	T
832.29	251.282	1.2038	0.00328862	t
968.555	275.782	1.21522	0.00279212	T
1104.82	300.786	1.22705	0.00242016	T
1241.08	326.335	1.2393	0.0021319	t
1377.35	352.461	1.25198	0.00190265	t
1513.62	379.19	1.2651	0.00171659	T
1649.88	406.543	1.27866	0.00156311	Ī
1786.15	434.54	1.29268	0.00143482	T
1922.41	463.201	1.30716	0.00132638	T
2058.67	492.541	1.32211	0.00123387	t
2194.94	522.578	1.33752	0.0011543	t
2331.2	553.326	1.35342	0.00108538	t
2467.47	584.803	1.36979	0.00102529	Ť
2603.74	617.022	1.38666	0.000972594	T
2740	650	1.40401	0.00092613	I
				İ
4	""			+

Figure 2.2: PVT Input Table

Figure 2.2 shows the input table for the fluid PVT properties of the desired reservoir to be studied. Data input for the reservoir pressure, solution gas/oil ratio, oil formation volume factor and gas formation volume factor can be seen. Other inputs still in this interface are the gas viscosity and oil viscosity.

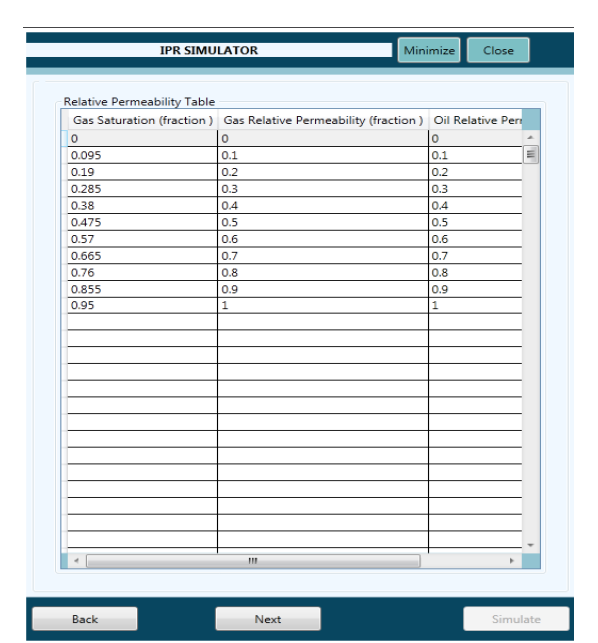


Figure 2.3: Relative Permeability Input Interface

Fig. 2.3 shows the interface that collects data for oil relative permeability and gas relative permeability. It also shows the gas saturation values for each of the

relative permeability input for both oil and gas.

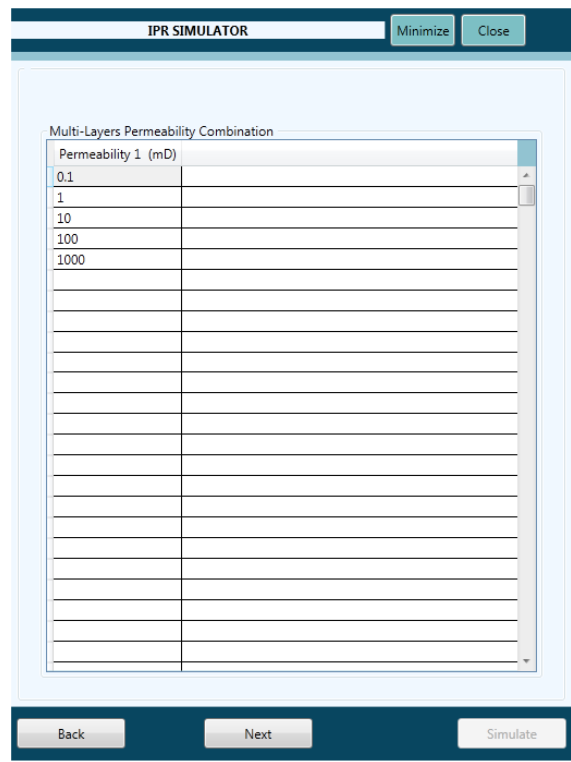


Figure 2.4: Permeability Input for the Multi-Layered Reservoirs

Fig. 2.4 shows the input interface for the permeability combination of the number of reservoir layers to be considered.

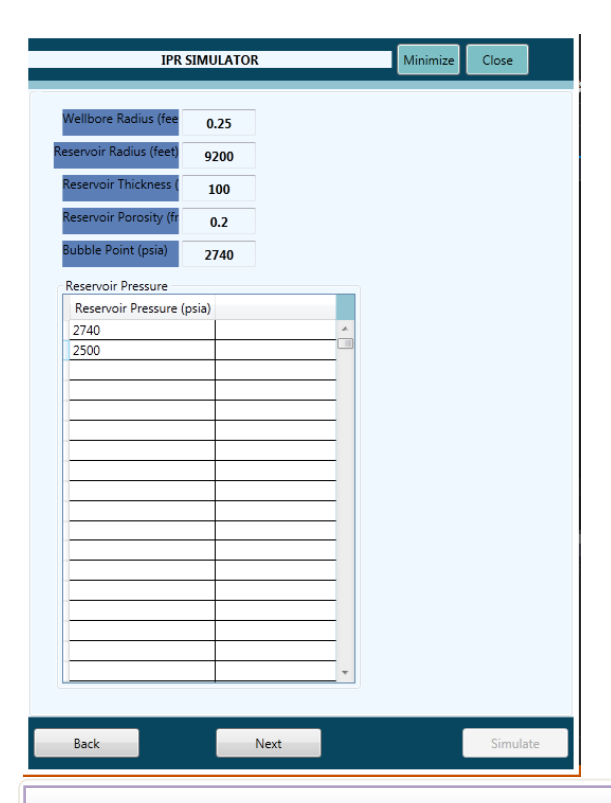


Figure 2.5: Input Reservoir Pressure

Fig. 2.5 shows the interface to input the pressure history of the reservoir to be simulated.

III. RESULTS AND DISCUSSIONS

3.1. Simulation of Computer Program with Real Data

The in-built wellbore radius for the simulator is 0.25ft, reservoir radius is 9,200ft, thickness of the reservoir is 100ft, porosity (assumed to be constant throughout all reservoir sections) is 20% and the simulator bubble-point pressure is assumed to be at 2,740 psia.

3.2. Data Presentation

Table 3.1: Reservoir Fluid Properties

P (psia)	Rs (SCF/SRB)	Bo (bbl/STB)	Bg (SCF/bbl)	µо (ср)	µд (ср)	ρο(lb/ft^3)	ρg(lb/ft^3)
14.7	103.176	1.13912	0.201988	0.716678	0.0132526	46.0816	0.0471549
150.965	132.278	1.15112	0.0193907	0.687302	0.0133306	45.8422	0.491199
287.23	156.549	1.16143	0.0100493	0.66395	0.0134489	45.6347	0.9478
423.495	180.071	1.17165	0.00672216	0.642288	0.0135959	45.428	1.41691
559.76	203.539	1.18205	0.00501741	0.621599	0.0137681	45.2173	1.89833
696.025	227.229	1.19275	0.00398247	0.601621	0.0139641	45.001	2.39166
832.29	251.282	1.2038	0.00328862	0.582236	0.0141833	44.7785	2.89627
968.555	275.782	1.21522	0.00279212	0.563384	0.0144251	44.5496	3.41129
1104.82	300.786	1.22705	0.00242016	0.545038	0.0146895	44.3143	3.93557
1241.08	326.335	1.2393	0.0021319	0.527184	0.0149759	44.0728	4.4677
1377.35	352.461	1.25198	0.00190265	0.509817	0.015284	43.8254	5.00602
1513.62	379.19	1.2651	0.00171659	0.492936	0.0156132	43.5724	5.54862
1649.88	406.543	1.27866	0.00156311	0.476543	0.0159625	43.3141	6.09344
1786.15	434.54	1.29268	0.00143482	0.460641	0.0163309	43.0507	6.63829
1922.41	463.201	1.30716	0.00132638	0.445234	0.016717	42.7828	7.18098
2058.67	492.541	1.32211	0.00123387	0.430325	0.0171193	42.5107	7.71938
2194.94	522.578	1.33752	0.0011543	0.415917	0.0175361	42.2347	8.25148
2331.2	553.326	1.35342	0.00108538	0.402013	0.0179656	41.9552	8.77546
2467.47	584.803	1.36979	0.00102529	0.388615	0.0184062	41.6726	9.28977
2603.74	617.022	1.38666	0.000972594	0.375723	0.0188561	41.3874	9.7931
2740	650	1.40401	0.00092613	0.363339	0.0193134	41.0998	10.2844

Table 3.1 reports the black oil PVT properties used in the simulation run of the developed computer program. As can be seen from the table, properties of both oil and gas are reported since the reservoir being modelled is assumed to be a solution gas-drive reservoir.

Table 3.2: Gas-Oil System Relative Permeabilities

Tuest 8:2: Gus Gil System Iterative I erinteuerinise					
Sg	Krg	Kro			
0	0	0			
0.095	0.1	0.1			
0.19	0.2	0.2			
0.285	0.3	0.3			
0.38	0.4	0.4			
0.475	0.5	0.5			
0.57	0.6	0.6			
0.665	0.7	0.7			
0.76	0.8	0.8			
0.855	0.9	0.9			
0.95	1	1			

Table 3.2 shows the relative permeability values for both oil and gas at different gas saturations in the reservoir.

Table 3.3: Permeabilities of different layer combinations

Case Number	k1 (mD)	
1	0.1	
2	1	
3	10	
4	100	
5	1000	

Table 3.3 shows the various permeability combinations of layers used in running the program.

3.3. Results obtained from Simulated Reservoir Properties

At the end of the program run, values of the ratio between production rate, $q_{\rm o}$ and absolute open flow potential (AOFP), $q_{\rm max}$ were obtained. These values were obtained for various ratios of wellbore flowing pressure, $P_{\rm wf}$ to reservoir pressure, $P_{\rm r}$. The simulated results yielded these output for the various permeability layer combinations reported in Table 3.3.

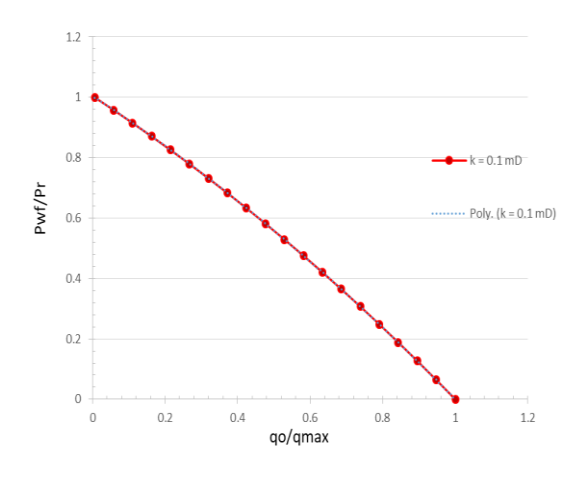


Figure 3.1: IPR Curve for permeability layer combination (k = 0.1 mD, Pr/Pb = 0.9124)

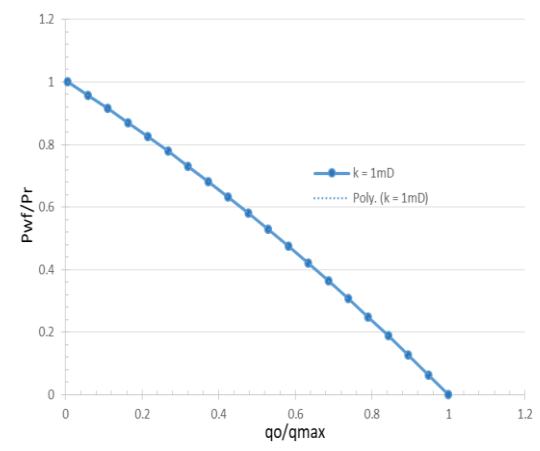


Figure 3.2: IPR Curve for permeability layer combination (k = 1 mD, Pr/Pb = 0.9124)

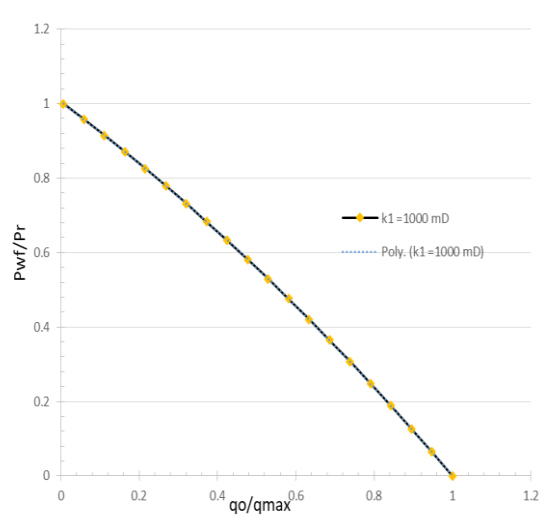


Figure 3.3: IPR Curve for permeability layer combination (k = 10 mD, Pr/Pb = 0.9124)

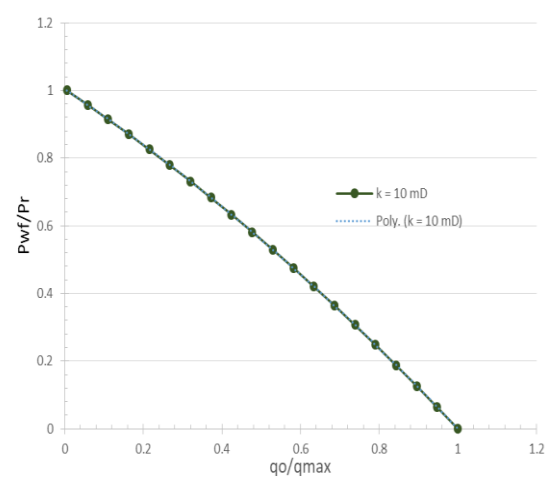


Figure 3.4: IPR Curve for permeability layer combination (k = 100 mD, Pr/Pb = 0.9124)

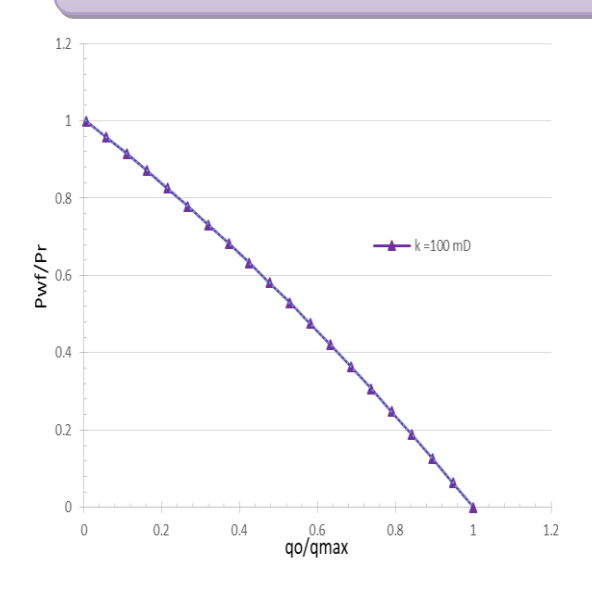


Figure 3.5: IPR Curve for permeability layer combination (k = 1000 mD, Pr/Pb = 0.9124)

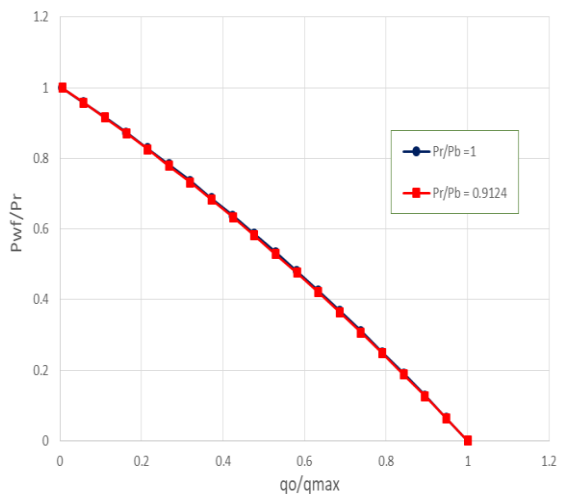


Figure 3.6: Comparison of IPR curves for various values of reservoir pressure ratios (k = 1,000 mD, Pr/Pb = 1 and Pr/Pb = 0.9124)

Table 3.4: Variation of Coefficients 'a' And 'b' With Permeability Combinations of Various Reservoir Layers, k

k values (mD)	Coefficient 'a'	Coefficient 'b'
0.1	0.236524332	0.763475668
1	0.23652434	0.76347566
10	0.23652434	0.76347566
100	0.23652434	0.76347566
1000	0.23652434	0.76347566

Table 3.4 shows the various coefficients obtained from the simulated results. These coefficients are rigorously analysed and the best fit for the IPR curves of Figures 4.1 through 4.5 is given as:

$$\frac{q_o}{q_{max}} = 1 - 0.24 \left(\frac{P_{wf}}{P_r}\right) - 0.76 \left(\frac{P_{wf}}{P_r}\right)^2$$
 (3.1)

(3.1) is a novel IPR correlation and can be used to obtain the AOFP and future production rates of wells producing from multi-layered reservoirs. Section 3.4 handles the sensitivity analysis of the developed correlation (3.1) and already established Qasem's correlation with real field data. Section 3.4 also looks at comparison of the model effectiveness when compared to Vogel's correlation and Qasem's correlation in predicting flow through a vertical well.

3.4. Field Case

3.4.1. Field Case Study - Well 6, Field A

Field A is solution gas-drive carbonate reservoir; the average gas saturation at the time of the tests was between 10 and 12%. The test consists of seven individual flows, the first four flow rates were run in a normal increasing sequence followed by reducing rate and then increasing rate. Table 3.5 gives the basic reservoir data for Field A.

Table 4.5: Field Case 1 – Well 6, Field A Basic Reservoir Data

Reservoir Pressure	1345 (psia)
Stabilized Production Rate	500 (STB/Day)
Bubble Point Pressure	2020 (psia)

Table 4.6: Comparison of Production Rates
Predicted from Different IPR Correlations and the
New Correlation

Field Data		New Correlation	Qasem's Correlation	Vogel's Correlation	
Pwf (psia)	qo (STB/Day)	qo (STB/Day)	qo (STB/Day)	qo (STB/Day)	
1345	0	-0.021906117	0	-2.43207E-14	
1242	66	57.18746439	53.07004495	58.33698736	
1178	93	90.75858932	84.41485523	92.51441678	
1123	134	118.3984611	110.3531798	120.6175541	
921	229	210.3121372	197.6966474	213.7743961	
719	321	287.1347083	272.5885451	291.1197208	
638	341	313.7008343	299.1219135	317.6931081	
400		377.7196888	365.5001437	381.0630803	
200		415.3178885	407.914353	417.3426929	
0		438.1223375	483.2585122	427.2129286	
	Average Absolute Errors	9.02%	14.58%	7.49%	

Table 3.6 shows various production rates predicted by different IPR correlations. A graphical comparison of the tabulated results is shown in Figure 3.7.

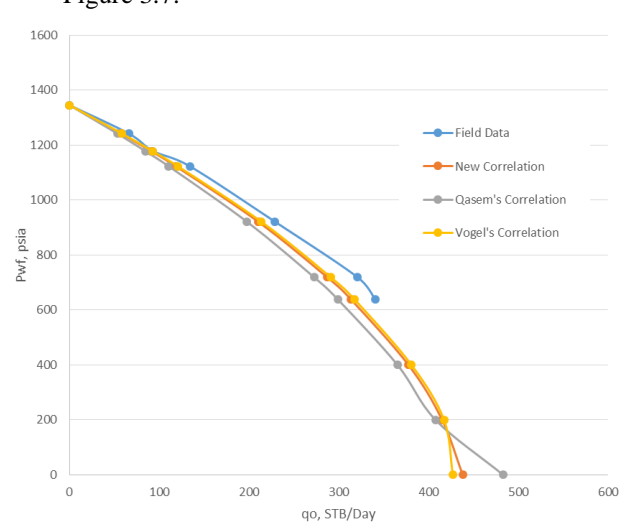


Figure 3.7: IPR Comparison for Field Case

From Figure 3.7 and Table 3.6, we can observe that the IPR for the new correlation is not too far away from actual values as it has an average absolute error value of about 9.02%. However, Vogel's IPR and Qasem's IPR have absolute errors of 14.58% and 7.49% respectively.

IV. CONCLUSION

4.1. Conclusion

- From the results obtained in Section 3.4, the proposed correlation showed good accuracy compared to the already existing correlations in predicting production rate data of the Field Case.
- The most important attribute of the new correlation is the fact that it takes into account several reservoir rock and fluid properties.
 These rock and fluid properties highly affected the IPR modelling process.
- Fluid flow between the reservoir layers causes the shape of the IPR to behave as if it were that of a homogenous reservoir.
- Changes in the IPR shapes can be observed with the decline of reservoir pressure.

4.2. Recommendations

- Composite IPR modelling should be extended to other reservoir types such as gas-condensate reservoirs and dry gas reservoirs in further study.
- More deployment of field data is required for further validation and tuning of the new correlation developed in this study.
- In order to extend the adaptability of the model developed in this work, more research should be done on this subject. The influence of an external reservoir boundary was not accounted for in this work and should be looked into in subsequent studies.

REFERENCES

- [1] M.J. Fetkovich, The isochronal testing of oil wells, *Annual Technical Conference & Exhibition*, Las Vegas, USA, 1973, SPE 4529.
- [2] A.M.Daoud, M.A. Salam, A.A.Hashem, and M.H. Sayyo, Inflow Performance Relationship Correlation for Solution Gas-Drive Reservoirs Using Non-Parametric Regression Technique, *The Open Petroleum Engineering Journal*, 10, 2017 152-156.
- [3] B. Milad, F. Civan, D. Devegowda and R.F. Sigal, Modeling and Simulation of Production from Commingled Shale Gas Reservoirs, Unconventional Resources Technology

- Conference, Denver, USA, 2013, SPE 168853.
- [4] B. Guo, K. Ling and A. Ghalambor, A Rigorous Composite IPR-Model for Multilateral Wells, Annual Technical Conference & Exhibition, San Antonio, USA, 2006, SPE 100923.
- [5] M. Elias, A.H. El-Banbi, K.A. Fattah and E.A.M. El-Tayeb, New Inflow Performance Relationship for Solution-Gas Drive Oil Reservoirs, Annual Technical Conference & Exhibition, New Orleans, USA, SPE 124041.
- [6] F. Qasem, A. Malallah, I.S. Nashawi and M. Mir, Modelling Inflow Performance Relationships for Wells Producing from Multi-layer Solution-gas Drive Reservoirs, North Africa Technical Conference & Exhibition, Cairo, EGY, SPE 149858.